

Dielectric and piezoelectric properties of $(K_{0.5}Na_{0.5})NbO_3$ – $Ba(Zr_{0.05}Ti_{0.95})O_3$ lead-free ceramics

Dunmin Lin,^{a)} K. W. Kwok, and H. W. L. Chan

Department of Applied Physics, The Hong Kong Polytechnic University, Kowloon, Hong Kong, China
and Materials Research Centre, The Hong Kong Polytechnic University, Kowloon, Hong Kong, China

(Received 4 August 2007; accepted 17 September 2007; published online 4 October 2007)

Lead-free ceramics $(1-x)(K_{0.5}Na_{0.5})NbO_3-xBa(Zr_{0.05}Ti_{0.95})O_3$ doped with 1 mol % MnO_2 have been fabricated by pressureless sintering. With the MnO_2 doping, all the ceramics can be well sintered at 1100–1160 °C and exhibit a dense and pure perovskite structure. After the addition of $Ba(Zr_{0.05}Ti_{0.95})O_3$, a relax behavior is induced and both the cubic-tetragonal and tetragonal-orthorhombic phase transitions shift to lower temperatures. Coexistence of the orthorhombic and tetragonal phases is hence formed in the ceramics with $0.04 < x < 0.07$ at room temperature. It is suggested that owing to the more possible polarization states resulting from the coexistence of the two phases, the piezoelectric and dielectric properties of the ceramics are enhanced significantly. The ceramic with $x=0.06$ exhibits the following optimum properties: $d_{33}=234$ pC/N, $k_p=0.49$, $k_t=0.48$, $\epsilon_r=1191$, $\tan \delta=1.20\%$, and $T_C=318$ °C. © 2007 American Institute of Physics. [DOI: 10.1063/1.2794798]

Among various lead-free piezoelectric ceramics, $K_{0.5}Na_{0.5}NbO_3$ (KNN) is considered a promising candidate because of its high Curie temperature (420 °C) and large electromechanical coupling factors.^{1,2} However, it is very difficult to obtain dense KNN ceramics using ordinary sintering process because of the high volatility of alkaline elements at high temperatures. A number of studies have been carried out to improve the sinterability and electrical properties of KNN ceramics; these include the formation of solid solutions of KNN with other ABO_3 perovskites^{3–7} and the use of sintering aids.⁸ In this letter, we report the preparation of a solid solution $(1-x)(K_{0.5}Na_{0.5})NbO_3-xBa(Zr_{0.05}Ti_{0.95})O_3$ (KNN-BZT- x) doped with 1 mol % MnO_2 by pressureless sintering and the resulting improvements in both densification and piezoelectric properties of the ceramics. $Ba(Zr_{0.05}Ti_{0.95})O_3$ ceramic is a perovskite ferroelectric exhibiting a large remanent polarization ($P_r=13$ – 18 $\mu C/cm^2$) and a high d_{33} (236 pC/N).⁹ These would be advantageous to the improvement of the piezoelectric properties. On the basis of our previous work,¹⁰ MnO_2 is added in order to improve the densification of the ceramics.

To prepare the KNN-BZT- x ceramics, KNN and BZT powders were first synthesized at 880 °C for 6 h and 1200 °C for 8 h, respectively, by a solid state reaction. After the calcination, KNN, BZT, and MnO_2 powders were weighted according to the formulas and then ball milled for 8 h. The resulting powders were mixed with a polyvinyl alcohol binder solution and then pressed into disk samples. The disk samples were sintered at 1100–1160 °C for 4 h in air. After the deposition of silver electrodes, the ceramics were poled under a dc field of 5–6 kV/mm at 180 °C in a silicone oil bath for 30 min. The piezoelectric properties of the ceramics, such as the piezoelectric coefficient d_{33} and the electromechanical coupling factors k_p and k_t , were then evaluated. d_{33} was measured at 60 Hz using a piezo- d_{33} meter (ZJ-3A, Institute of Acoustics Academia Sinica), while

k_p and k_t were determined by the resonance method according to the IEEE Standards 176 using an impedance analyzer (4294A, Agilent).

Figure 1 shows, as examples, the scanning electron microscopy (SEM) micrographs of the KNN-BZT-0.06 ceramics without and with MnO_2 doping. It has been observed that the ceramics without MnO_2 doping are generally porous and electrically conductive. After the doping of 1 mol % MnO_2 , all the ceramics can be well sintered at a relatively low temperature and have a dense structure, giving a relatively high density ($>97\%$) and resistivity ($>10^{10}$ Ω cm).

Figure 2 shows the X-ray diffraction (XRD) patterns of the KNN-BZT- x ceramics. All the ceramics possess a pure perovskite structure and no secondary phase is observed

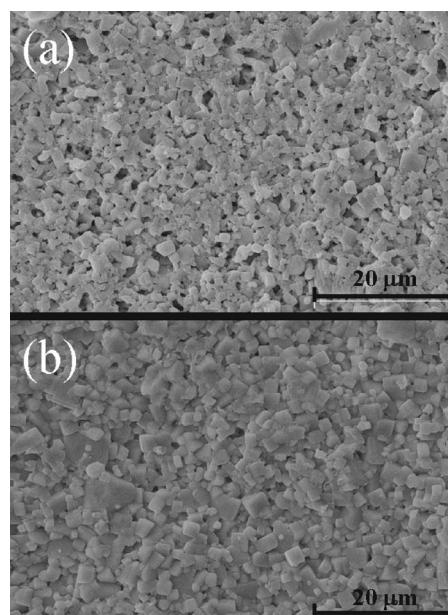


FIG. 1. SEM micrographs of the KNN-BZT-0.06 ceramics (a) without MnO_2 doping, sintered at 1170 °C for 4 h, and (b) with 1 mol % MnO_2 doping, sintered at 1140 °C for 4 h.

^{a)}Electronic mail: ddmd222@yahoo.com.cn

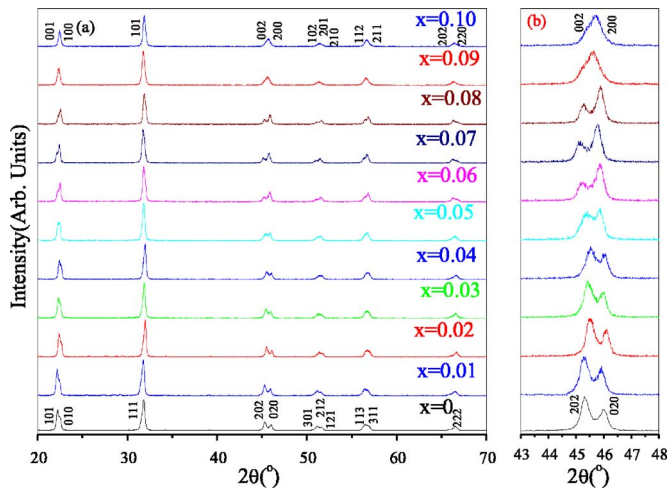


FIG. 2. (Color online) XRD patterns of the KNN-BZT- x ceramics.

[Fig. 2(a)]. This suggests that BZT has diffused into the KNN lattices to form a homogeneous solid solution. Together with the enlarged XRD patterns, as shown in Fig. 2(b), it can be seen that the ceramics with $x \leq 0.04$ have an orthorhombic structure (the corresponding XRD patterns can be indexed in Ref. 11). As x increases, a tetragonal phase appears and increases continuously in volume. At $x \geq 0.07$, the ceramic possesses the tetragonal phase only (the corresponding XRD patterns can be indexed in Ref. 12). These suggest that the orthorhombic and tetragonal phases coexist in the ceramics with $0.04 < x < 0.07$. At $x \geq 0.09$, the two diffraction peaks (002) and (200) near 46° become merged into a single peak. It seems that the ceramic has a tendency to transform into another phase, e.g., pseudocubic, at high concentrations of BZT. However, it is suggested that the ceramic should remain at the tetragonal phase, probably with similar lattice constants a , b , and c . This is similar to the results reported for the KNN-BaTiO₃ ceramics.¹³ Additional experimental data will be provided below for further discussion.

Figure 3(a) shows, as examples, the temperature dependences of the relative permittivity ϵ_r for the KNN-BZT- x ceramics with $x=0, 0.03, 0.06$, and 0.09 , while the variations of the phase transition temperatures with x are summarized in Fig. 3(b). The KNN-BZT-0.00 ceramic exhibits the classic ferroelectric characteristics, undergoing the cubic-tetragonal phase transition at 424°C (T_C) and the tetragonal-orthorhombic phase transition at 203°C (T_{O-T}). After the addition of BZT, the ceramics exhibit similar temperature dependences of ϵ_r , but with the two transition peaks shifted to lower temperatures [Fig. 3(a) and the inset]. No other phase transition peaks have been observed at temperatures below T_{O-T} for each ceramic. The observed T_{O-T} for the ceramics with $x=0.09$ and 0.10 are about -38 and -50°C , respectively, suggesting that the ceramics are of tetragonal phase at room temperature [Fig. 3(b)]. This provides additional evidence for the suggestion that the ceramics with $x \geq 0.09$ should remain at the tetragonal phase although their room-temperature diffraction peaks (002) and (200) merge into one (Fig. 2). As shown in Fig. 3(b), the observed T_{O-T} for the ceramics with $0.04 < x < 0.07$ is close to room temperature. This suggests that the orthorhombic and tetragonal phases coexist in these ceramics, which is consistent with the results of x-ray diffraction (Fig. 2).

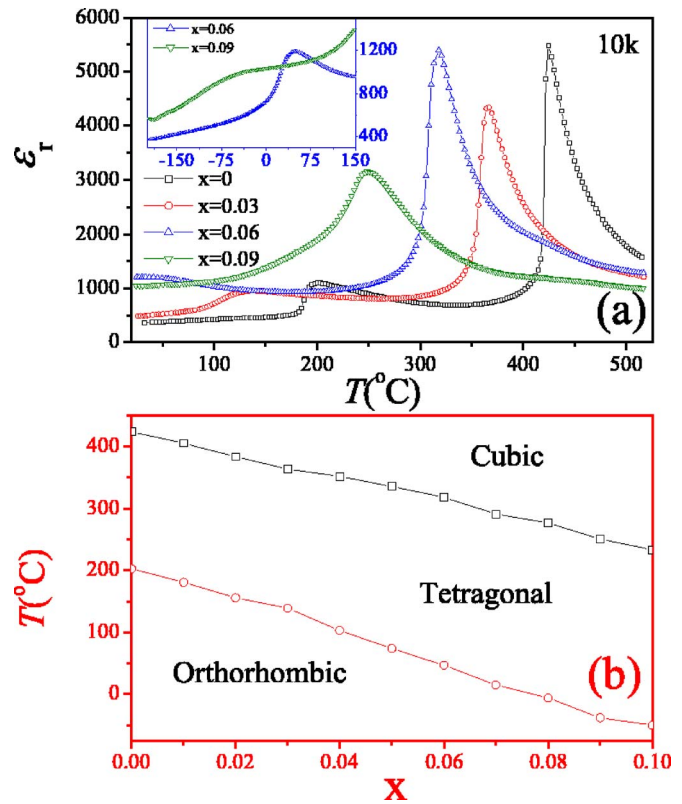


FIG. 3. (Color online) (a) Temperature dependences of ϵ_r for the KNN-BZT- x ceramics with $x=0, 0.03, 0.06$, and 0.09 at 10 kHz . The inset shows the dependences of ϵ_r for the ceramics with $x=0.06$ and 0.09 in the temperature range of -200 to 150°C ; (b) Phase diagram of the KNN-BZT- x ceramics.

As also shown in Fig. 3(a), the transition peak associated with the cubic-tetragonal phase transition becomes broadened gradually with increasing x . This suggests that a diffuse phase transition is induced and the ceramic transforms gradually from a normal ferroelectric to a relaxor ferroelectric. The diffuseness of a phase transition can be determined from the modified Curie-Weiss law, $1/\epsilon_r - 1/\epsilon_m = C^{-1}(T - T_m)^\gamma$,¹⁴ where ϵ_m is the maximum value of ϵ_r at the phase transition temperature T_m , γ is the degree of diffuseness, and C is the Curie-like constant. γ can have a value ranging from 1 for a normal ferroelectric to 2 for an ideal relaxor ferroelectric. Figure 4 shows the plots of $\ln(1/\epsilon_r - 1/\epsilon_m)$ vs $\ln(T - T_m)$ for the KNN-BZT- x ceramics with $x=0, 0.03, 0.06$, and 0.09 . All the samples exhibit a linear relationship. By least-squares fitting the experimental data to the modified Curie-Weiss law, γ was determined. The calculated γ for the ceramics with $x=0$ and 0.03 are 1.12 and 1.13 , respectively, suggesting that they are normal ferroelectrics. As x increases, γ increases gradually from 1.26 at $x=0.06$ to 1.63 at $x=0.09$, indicating that the ceramic has transformed gradually from a normal ferroelectric to a relaxor ferroelectric. For the KNN-BZT- x ceramics, Ba²⁺ (ion radius of 1.34 \AA) substitutes the A-site Na⁺ and K⁺ (0.97 and 1.33 \AA , respectively), while Ti⁴⁺ (0.68 \AA) and Zr⁴⁺ (0.79 \AA) substitute the B-site Nb⁵⁺ (0.69 \AA). As the ions in each site have similar radii, the A-site and B-site disordered degrees and the local compositional fluctuation may increase,^{14,15} thus giving rise to a relaxor phase transition.

The variations of d_{33} , k_p , k_t , ϵ_r , and $\tan \delta$ with x for the KNN-BZT- x ceramics are shown in Fig. 5. The observed d_{33}

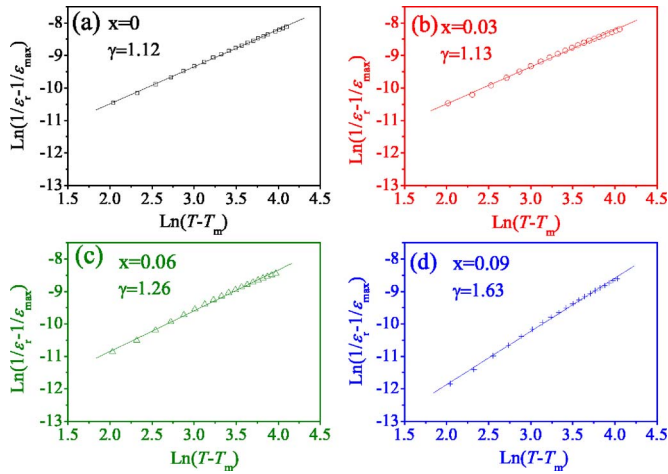


FIG. 4. (Color online) Plots of $\ln(1/\epsilon_r - 1/\epsilon_m)$ vs $\ln(1/T - 1/T_m)$ for the KNN-BZT- x ceramics. The symbols denote the experimental data, while the solid lines denote the least-squares fitting line to the modified Curie-Weiss law.

increases with increasing x and then decreases, giving a maximum value of 234 pC/N at $x=0.06$. Similar to d_{33} , k_p and k_t reach the maximum values of 0.49 and 0.48, respectively, at $x=0.06$ [Fig. 5(a)]. On the other hand, ϵ_r increases with increasing x , while $\tan \delta$ remains almost unchanged at a value smaller than 4.5% [Fig. 5(b)].

For lead-based perovskite ceramics, such as $\text{Pb}(\text{Ti},\text{Zr})\text{O}_3$ (Ref. 16) and $\text{Pb}(\text{Mg}_{1/3}\text{Nb}_{2/3})\text{O}_3\text{-PbTiO}_3$,¹⁷ their piezoelectric properties become maximal near the mor-

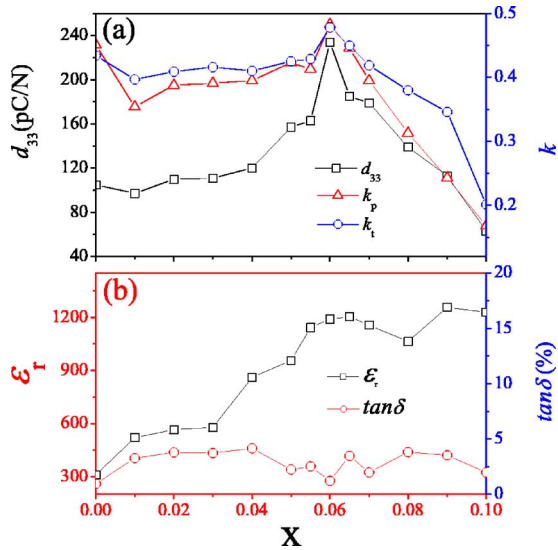


FIG. 5. (Color online) Variations of d_{33} , k_p , k_t , ϵ_r , and $\tan \delta$ with x for the KNN-BZT- x ceramics.

photropic phase boundary (MPB) region. It is normally believed that the ceramics near the MPB may contain both the rhombohedral and tetragonal phases and thus more possible polarization states, which consequently lead to the significant enhancement in the piezoelectric properties. Similarly, the optimum piezoelectric properties observed in the KNN-BZT- x ceramics with $0.04 < x < 0.07$ should result from the more possible polarization state resulting from the coexistence of the orthorhombic and tetragonal phases.

In conclusion, a KNN-BZT- x lead-free ceramic has been prepared by an ordinary sintering technique. After the addition of BZT, a relaxor behavior is induced and both T_C and T_{O-T} decrease. Accordingly, the ceramics with $0.04 < x < 0.07$ contain both the orthorhombic and tetragonal phases at room temperature. It is suggested that owing to the more possible polarization states resulting from the coexistence of the two phases, the KNN-BZT-0.06 ceramic exhibits the following optimum properties: $d_{33}=234$ pC/N, $k_p=0.49$, $k_t=0.48$, $\epsilon_r=1191$, $\tan \delta=1.20\%$, and $T_C=318$ °C.

This work was supported by the Research Grants Council of the Hong Kong Special Administrative Region (Project No. PolyU 5188/06E), the Niche Area Projects (1-BBZ3 and 1-BB95), and the Centre for Smart Materials of The Hong Kong Polytechnic University.

¹R. E. Jaeger and L. Egerton, J. Am. Ceram. Soc. **45**, 209 (1962).

²L. Egerton and D. M. Dillom, J. Am. Ceram. Soc. **42**, 438 (1959).

³H. Y. Park, C. W. Ahn, H. C. Song, J. H. Lee, S. Nahm, K. Uchino, H. G. Lee, and H. J. Lee, Appl. Phys. Lett. **89**, 062906 (2006).

⁴G. Z. Zang, J. F. Wang, H. C. Chen, W. B. Su, C. M. Wang, P. Qi, B. Q. Ming, J. Du, L. M. Zheng, S. Zhang, and R. T. Shrout, Appl. Phys. Lett. **88**, 212908 (2006).

⁵Y. Guo, K. Kakimoto, and H. Ohsato, Appl. Phys. Lett. **85**, 4121 (2004).

⁶E. Hollenstein, M. Davis, D. Damjanovic, and N. Setter, Appl. Phys. Lett. **87**, 182905 (2005).

⁷Y. Saito, H. Takao, T. Tani, T. Nonoyama, K. Takatori, T. Homma, T. Nagaya, and M. Nakamura, Nature (London) **432**, 84 (2004).

⁸M. Matsubara, K. Kikuta, and S. Hirano, J. Appl. Phys. **97**, 114105 (2005).

⁹Z. Zhi, C. Ang, R. Guo, and A. S. Bhalla, J. Appl. Phys. **92**, 1489 (2002).

¹⁰D. Lin, K. W. Kwok, H. Tian, and H. W. L. Chan, J. Am. Ceram. Soc. **90**, 1458 (2007).

¹¹International Centre for Diffraction Data, JCPDS-ICDD 2001, file No. 71-2171.

¹²International Centre for Diffraction Data, JCPDS-ICDD 2001, file No. 71-0945.

¹³C. W. Ahn, H. C. Song, S. Nahm, S. H. Park, K. Uchino, S. Priya, H. G. Lee, and N. K. Kang, Jpn. J. Appl. Phys., Part 2 **44**, L1361 (2005).

¹⁴K. Uchino and S. Nomura, Ferroelectr., Lett. Sect. **44**(3), 55 (1982).

¹⁵Y. Li, W. Chen, Q. Xu, J. Zhou, X. Gu, and S. Fang, Mater. Chem. Phys. **94**, 328 (2005).

¹⁶B. Jaffe, W. R. Cook, and H. Jaffe, *Piezoelectric Ceramics* (Academic, London, 1971), pp. 135–183.

¹⁷B. Noheda, D. E. Cox, G. Shirane, J. Gao, and Z. G. Ye, Phys. Rev. B **66**, 054104 (2002).

Applied Physics Letters is copyrighted by the American Institute of Physics (AIP). Redistribution of journal material is subject to the AIP online journal license and/or AIP copyright. For more information, see <http://ojps.aip.org/aplo/aplcr.jsp>